A proteome-wide screen identifies valosin-containing protein as an essential regulator of podocyte endoplasmic reticulum stress

HUANG ZhiYong[1†], HONG Quan[1†], XUE Peng[2], PAUL Goulding[3], FENG Zhe[1], WANG LiYuan[1], MEI Yan[1], WU LingLing[1], CHEN XiangMei[1*] & WU Di[1*]

[1] *State Key Laboratory of Kidney Disease (2011DAV00088), Kidney Department & Institute of Nephrology, Division of Clinical Internal Medicine, Chinese People's Liberation Army General Hospital, Beijing 100853, China;*
[2] *Laboratory of Proteomics, Institute of Biophysics, Chinese Academy of Sciences, Beijing 100101, China;*
[3] *Nonlinear Dynamics Ltd, Keel House, Garth Heads, Newcastle upon Tyne, NE1 2JE, UK*

To investigate proteins expressed in the renal tissue of the passive Heymann nephritis (pHN) rat model, we prepared pHN rat models with anti-FxA1 serum and analyzed the proteins differentially expressed in the kidney tissue with label-free liquid chromatography-tandem mass spectrometry. We then analyzed in depth the endoplasmic reticulum stress (ERS)-related protein using an online bioinformatics platform. Forty-one differential proteins and their annotations were obtained. Gene Ontology (GO) function analysis showed that 16 proteins were involved in cellular metabolism and 22 were proteins related to catalytic activity, including protein folding or ATPase. Protein-GO networks indicated that VCP could interact with the ERS marker HSPa5, with both involved in a single pathway. On inhibition of podocyte VCP by RNAi under normal conditions, the HSPa5 expression level did not change, but when the cell was subjected to ERS by tunicamycin, HSPa5 expression significantly increased with RNAi of VCP when compared with the tunicamycin-treated group. Our results showed that ERS plays an important role in podocyte injury of membranous nephropathy and is mediated by an HSPa5-VCP signaling pathway, in which the most predominant proteins are those related to cellular metabolism and catalytic activity.

passive Heymann nephritis, ER stress, valosin-containing protein, proteomic

Membranous nephropathy (MN), a common nephrotic syndrome in adults, is an important cause of chronic kidney disease [1,2]. The distinctive pathologic feature of MN is the presence of immune deposits beneath podocytes [3]. The mechanism of podocyte damage is thought to be quite complex, involving activation of complement and cytokines, oxidative stress, and autophagy. The passive Heymann nephritis (pHN) model is the most commonly used animal model to simulate the conditions of MN [4,5]. Although

previous studies have used the pHN model to analyze the mechanism of MN development at multiple sites, few have focused on the gene changes of the entire kidney. The current study therefore analyzed differentially expressed proteins of the pHN rat model with high-throughput technology.

In the past, mass spectrometry (MS) has been of little use in quantifying differential proteins, being limited to mainly qualitative research. Recently, however, comparative quantification of label-free liquid chromatography (LC)-MS proteomics data has emerged as an alternative approach [6]. Label-free quantification [7] MS can determine the differential expression of proteins. In this method, proteins are compared based on the intensities of extracted ion chroma-

tograms from complex samples such as enzymatic digests. This method does not require metabolic, chemical, or enzymatic labeling or premixing of the samples [8]. Multiple data sets, typically run in triplicate, are aligned using mass and LC elution time, which improves the sensitivity and accuracy of results when compared with the traditional two-dimensional technology [9–11]. Therefore, label-free quantification MS has the advantages of convenience and reliable protein quantification and identification.

This study on the pHN rat model used label-free quantitative MS for high-throughput identification of differentially expressed proteins at several time points. The endoplasmic reticulum stress (ERS)-related protein was then analyzed in depth using the online analysis platform found at http://www.uniprot.org and http://bioinfo.capitalbio.com/mas3.0/.

1 Materials and methods

1.1 Experimental animals

Nine 180–200 g male SD (Sprague-Dawley) rats were purchased from Beijing Huafukang Company and divided into three groups containing three animals each: control, 14 d postinjection, and 21 d postinjection. Experimental animals were housed under specific pathogen-free conditions: $22\pm1°C$, 40% humidity, 12-h:12-h light/dark cycle, and free access diet. The study was approved by the Institutional Animal Care and Use Committee at the Chinese PLA General Hospital and Military Medical Postgraduate College.

1.2 Reagents

Reagents used were acetonitrile (AN; Fisher Scientific, Waltham, MA, USA), formic acid (FA; Fisher Scientific), dithiothreitol (DTT; Sigma, St. Louis, MO, USA), iodoacetemide (IAA; Amresco, Solon, OH, USA), NH_4HCO_3 (Sigma), trypsin enzymolysis liquid (Promega, Madison, WI, USA), BCA protein concentration detection reagent kit (Pierce, Rockford, IL, USA), tunicamycin (Tm; Sigma), rabbit polyclonal anti-HSPa5, VCP antibody (Santa Cruz Biotechnology, Santa Cruz, CA, USA), and anti-rabbit IgG (Santa Cruz Biotechnology).

1.3 Preparation and confirmation of PHN model

Tubular brush border extracts and anti-Fx1A serum was prepared according to the literature [12–14]. Antisera at 1 mL/100 g (titer 1:250) were given as an initial tail vein injection, followed by a second dose 1 h later and one further booster injection. The control group received intravenous injection of the same dose of saline. All pHN rats had heavy proteinuria (urine protein >100 mg/d; normal <20). At 14 and 21 d after injection, rats were anesthetized by intraperitoneal injection of 2% sodium pentobarbital (40 mg/kg) prior to collection of kidney tissue samples.

1.4 Cell culture and siRNA transfection

Preserved mouse podocytes (MPCs) provided by Dr. Peter Mundel (University of Miami, Miami, FL, USA) were cultured as described previously [15]. Differentiated podocytes were treated with 2.5 ng/mL Tm (Sigma) for 10 h to induce the ERS.

siRNA-targeting VCP was purchased from Santa Cruz Biotechnology (cat. sc-37188). The siRNA was transfected into MPCs by Jetprime Polyplus transfection reagent (Polyplus-transfection Inc., New York, NY, USA) according to the manufacturers' recommendations.

1.5 Protein preparation

Kidney tissues were lysed in buffer solution (50 mmol/L Tris-HCl (pH 7.6), 150 mmol/L NaCl, 1% NP-40, 0.1% sodium dodecyl sulfate (SDS), 0.5% deoxycholic acid, 1 μg/mL leupeptin, 1 μg/mL aprotinin, and 0.5 mmol/L phenylmethylsulfonyl fluoride), then cooled on ice for 30 min prior to centrifuging at 12000 r/min for 30 min at 4°C. The supernatant was removed and the protein concentration was determined by the BCA method (Bio-Rad, Hercules, CA, USA). Then 10 mmol/L DTT was incubated with 100 μg protein at 56°C for 1 h. After cooling to room temperature, the protein was alkalized by 50 mmol/L IAM in darkness for 45 min. Excess IAM was removed with 40 mmol/L DTT at room temperature. The sample was further diluted five times with 25 mmol/L NH_4HCO_3. Trypsin 1% was added to digest the protein for 12 and 6 h at 37°C. FA 0.1% was used to terminate digestion, and the debris was removed by centrifugation at 13000 r/min for 10 min. The supernatant was stored at −80°C for MS analysis.

1.6 LC-MS analysis

The multidimensional protein identification system is composed of an LTQ-ion trap (ThermoFisher Scientific, Waltham, USA) mass spectrometer with an electrospray ionization (nano-ESI) source. We have performed LC-MS analysis previously [16]. Briefly, 100 μg of digested peptides were pre-fractionated then were injected onto a self-made biphasic capillary column by high-pressure nitrogen. The mobile phase consists of three solutions: A (5% AN, 0.1% FA), B (80% AN, 0.1% FA), and C (800 mmol/L ammonium acetate, 5% AN, 0.1% FA). Solution A was used to desalt the biphasic capillary column for 45 min, after which solution C was used to wash it stepwise, with the concentration of ammonium acetate increasing from 0 to 800 mmol/L. The elution from the column was loaded onto a C18 analytical capillary chromatography column and a fraction from the column was ionized by electrospray for MS analysis. The spray voltage was set to 2.0 kV, and the temperature of the heated capillary was set to 200°C. MS data were collected in a data-dependent acquisition mode. Parameters

related to MS/MS data acquisition were set as follows: normalized collision energy 35%, ion selection threshold 200 counts, activation Q 0.250, activation time 30 ms, and dynamic exclusion time 30 s. The elution gradient of HPLC and MS scanning were controlled by XCalibur (Fisher Scientific).

1.7   Data processing and protein identification

LC-MS data were processed using Progenesis LC‑MS software (Nonlinear Dynamics Corp., Newcastle upon Tyne, UK) using the default settings. Proteins were identified using the NCBI rat database (March 2011). The GI number of proteins was transformed into UniProtKB on http://www.uniprot.org [17]. Pathway networks and protein functional grouping were generated by the online platform at http://bioinfo.capitalbio.com/mas3.0/.

1.8   Western blotting

Fifty micrograms of total protein was separated by 7.5% SDS-PAGE, transferred to a membrane, and blocked with 5% skim milk, probed with primary antibody for 2 h at room temperature, and incubated with horseradish peroxidase-conjugated secondary antibody. β-actin was used for the sample control. Immunoreactive bands were visualized using an enhanced chemiluminescent system.

1.9   Real-time PCR assay

RNA was extracted from tissues and cells using TRIzol reagent (Invitrogen, Carlsbad, CA, USA) and was reverse transcribed to cDNA using M-MLV reverse transcriptase (2 μg) (Invitrogen). The cDNA was used as a template in quantitative real-time PCR reactions performed using TaqMan PCR Master Mix and an ICycler system (Bio-Rad). The following primers and probe were designed from the full-length *VCP* mRNA sequence and synthesized by SBS Biotechnology Corp. (Beijing, China): sense, 5′-AAACC-GTGGTAGAGGTGCCA-3′; antisense, 5′-CTTGGAAGG-TGTCATGCCAA-3′; and TaqMan probe, 5′-FAMCAGT-ATCCTGTGGAGCACCCAGACAAATTCTAMRA-3′. As an internal control, rat *GAPDH* was amplified using the following: sense, 5′-GGCATGGACTGTGGTCATGAG-3′; antisense, 5′-TGCACCACCAACTGCTTAGC-3′; and TaqMan probe, FAM-5′-CCTGGCCAAGGTCATCCATGACA-ACTTTAMRA-3′. Relative expression (fold-change vs. control) was quantified by the $2^{-\Delta\Delta C_t}$ method [18].

1.10   Statistical processing

All data were analyzed using SPSS 13.0 (SPSS Inc., Chicago, IL, USA) software; data are expressed as the mean ± SD. The differences between the two groups were compared with ANOVA, and $P < 0.05$ was considered statistically significant.

2   Results

2.1   LC-MS analysis results

There were 2134 total proteins and 234 differentially expressed proteins in all three experimental groups. Of those, 41 had 20 > NRatio > 1.5 (upregulation) or 0.05 < NRatio < 0.66 (downregulation) (NRatio: the change ratio of the up/down-regulated protein on day 14 or 21 versus control). Five proteins have not been annotated in the Uniprot database, including rCG25753 isoform CRA_b, rCG53940 isoform CRA_a, aldolase B isoform CRA_a, rCG55135 isoform CRA_c, and alanine-glyoxylate aminotransferase 2 isoform CRA_c, and 36 proteins have the corresponding Uniprot ID. Table 1 shows how the proteins were grouped.

2.2   Classification of differentially expressed proteins

All differentially expressed proteins, upregulated or downregulated at day 14 or 21, were classified into three groups, A, B, and C. Proteins in group A were downregulated at day 14, but upregulated at day 21; group B showed downregulation at days 14 and 21; and group C showed upregulation at days 14 and 21. As shown in Figure 1, group A contained UK114, B4F768, CALB1, THIM, OAT, COTL1, Q68FT4, ACTN4, DECR, D3ZZN3, Q66HT1, Q63011, ACON, Q3MHS9, HSP7C, ADT2, Q6AYS2, and Q7TMC7; group B contained DCXR, GSH0, GRP75, Q9QYA6, ATPB, XYLB, G3V826, GRP78g and GSH1; and group C contained NIT2, IDHC, AATC, Q7TP54, TERA, ST1C2, D4A2K1, AASS, and GSHR.

2.3   Gene Ontology analysis of differentially expressed proteins

Differentially expressed proteins were analyzed according to the Gene Ontology (GO) classification. As shown in Figure 2(a), among these proteins, 23 contributed to cellular structure, 30 to molecular function, and 22 to biological processes. The subgroup analysis is shown in Figure 2(b)–(d). In the biological process category, proteins related to cellular processes have the highest incidence with 19 proteins. In this subgroup, 16 proteins are involved in cellular metabolic processes, as shown in Table 2. Other biological processes included those of multicellular organisms, e.g. biological regulation and response to stimuli. The proteins related to cell structure include those needed to build, e.g. organelles and macromolecules. Of the proteins related to molecular function, most are related to catalytic activity (22 proteins); details are listed in Table 3. Other proteins are related to binding or oxidoreductase activity function.

Table 1 Protein annotation of PHN model

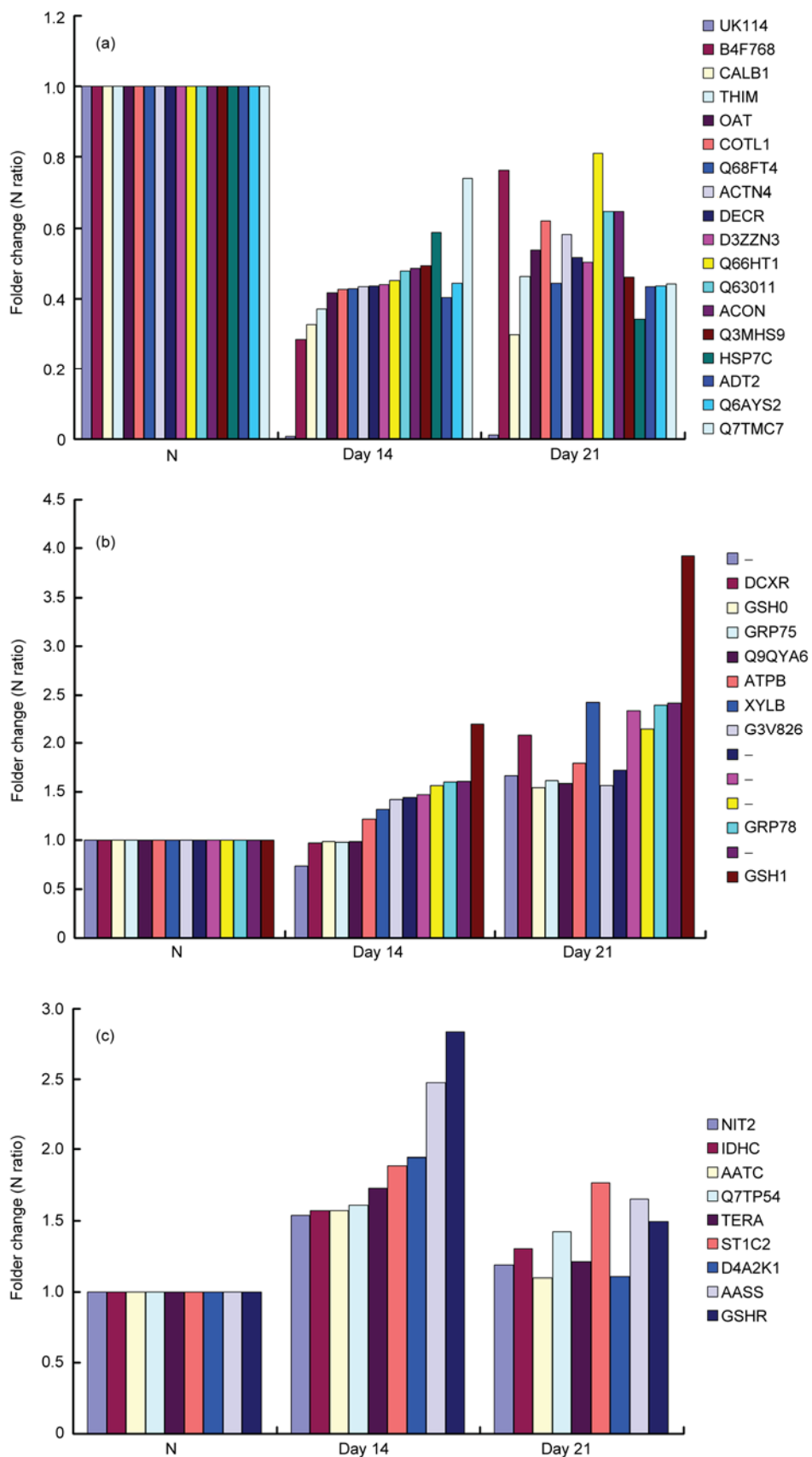| Cat.	Accession	Uniprot AC	Protein name	Gene name	Description	Folder change ratio 14 d/N	21 d/N
A	gi|4456766	P52759	UK114	*Hrsp12, Psp1*	perchloric acid soluble protein	0.0074	0.0108
	gi|195540087	B4F768	B4F768	*Aldh4a1 LOC641316*	Aldh4a1 protein	0.2834	0.7630
	gi|203237	P07171	CALB1	*Calb1*	calbindin-d28k	0.3257	0.2984
	gi|18426866	P13437	THIM	*Acaa2*	3-ketoacyl-CoA thiolase, mitochondrial	0.3699	0.4622
	gi|11968102	P04182	OAT	*Oat*	ornithine aminotransferase, mitochondrial precursor	0.4172	0.5379
	gi|157823483	B0BNA5	COTL1	*Cotl1, Clp*	coactosin-like protein	0.4255	0.6209
	gi|51260799	Q68FT4	Q68FT4	*Suclg2*	Suclg2 protein	0.4286	0.4441
	gi|6636119	Q9QXQ0	ACTN4	*Actn4*	alpha-actinin 4	0.4337	0.5823
	gi|37748456	Q64591	DECR	*Decr1, Decr*	2,4-dienoyl CoA reductase 1, mitochondrial	0.4360	0.5160
	gi|157818027	D3ZZN3	D3ZZN3	*Acss1, rCG_37494*	acetyl-coenzyme A synthetase 2-like, mitochondrial	0.4393	0.5023
	gi|158081751	Q66HT1	Q66HT1	*Aldob, rCG_60366*	fructose-bisphosphate aldolase B	0.4505	0.8098
	gi|802111	Q63011	Q63011	*MGC72973*	zero beta-globin	0.4773	0.6468
	gi|40538860	Q9ER34	ACON	*Aco2*	aconitate hydratase, mitochondrial precursor	0.4863	0.6475
	gi|76253725	Q3MHS9	Q3MHS9	*Cct6a, rCG_21714*	T-complex protein 1 subunit zeta	0.4927	0.4606
	gi|13242237	P63018	HSP7C	*Hspa8, Hsc70 Hsc73*	heat shock cognate 71 kD protein	0.5872	0.3419
	gi|32189350	Q09073	ADT2	*Slc25a5, Ant2*	ADP/ATP translocase 2	0.4028	0.4346
	gi|58865994	Q6AYS2	Q6AYS2	*Sfxn1, rCG_24191*	sideroflexin-1	0.4429	0.4360
	gi|33086606	Q7TMC7	Q7TMC7	*Tf Srprb*	Ab2-417	0.7389	0.4420
B	gi|149019103	–	–	–	rCG25753, isoform CRA_b	0.7333	1.6667
	gi|19705501	Q920P0	DCXR	*Dcxr, Glb*	*L*-xylulose reductase	0.9750	2.0833
	gi|8393446	P48508	GSH0	*Gclm, Glclr*	glutamate—cysteine ligase regulatory subunit	0.9856	1.5379
	gi|1000439	P48721	GRP75	*Hspa9, Grp75 Hspa9a*	grp75	0.9776	1.6098
	gi|6523793	Q9QYA6	Q9QYA6	*Slc4a4, nbc*	electrogenic Na$^+$ bicarbonate cotransporter	0.9900	1.5812
	gi|203033	P10719	ATPB	*Atp5b*	F1-ATPase beta subunit	1.2185	1.7899
	gi|76096348	Q3MIF4	XYLB	*Xylb*	xylulose kinase	1.3200	2.4300
	gi|149034221	G3V826	G3V826	*Tkt, rCG_42377*	transketolase, isoform CRA_a	1.4193	1.5625
	gi|149055818	–	–	–	rCG53940, isoform CRA_a	1.4390	1.7236
	gi|149020188	–	–	–	aldolase B, isoform CRA_a	1.4711	2.3388
	gi|149045753	–	–	–	rCG55135, isoform CRA_c	1.5639	2.1504
	gi|25742763	P06761	GRP78	*Hspa5, Grp78*	78 kD glucose-regulated protein precursor	1.5961	2.3973
	gi|149027328	–	–	–	alanine-glyoxylate aminotransferase 2, isoform CRA_c	1.6021	2.4187
	gi|25742748	P19468	GSH1	*Gclc, Glclc*	glutamate—cysteine ligase catalytic subunit	2.2046	3.9274
C	gi|77628000	Q497B0	NIT2	*Nit2*	omega-amidase NIT2	1.5374	1.1864
	gi|13928690	P41562	IDHC	*Idh1*	isocitrate dehydrogenase [NADP] cytoplasmic	1.5688	1.3028
	gi|220684	P13221	AATC	*Got1*	cytosolic aspartate aminotransferase	1.5696	1.0949
	gi|110625641	Q7TP54	Q7TP54	*Fam65b, RGD1306939*	family with sequence similarity 65, member B	1.6062	1.4191
	gi|17865351	P46462	TERA	*Vcp*	transitional endoplasmic reticulum ATPase	1.7281	1.2094
	gi|71896574	Q9WUW8	ST1C2	*Sult1c2 Sultk1*	sulfotransferase 1C2	1.8846	1.7668
	gi|157822207	D4A2K1	D4A2K1	*Hoga1, RGD1310475_predicted rCG_57749*	dihydrodipicolinate synthase-like, mitochondrial	1.9459	1.1041
	gi|155369281	A2VCW9	AASS	*Aass*	alpha-aminoadipic semialdehyde synthase, mitochondrial precursor	2.4768	1.6490
	gi|1657632	P70619	GSHR	*Gsr*	glutathione reductase	2.8381	1.4945

Figure 1   All differentially expressed proteins were divided into three categories. (a) The expression of proteins was downregulated at day 14, but upregulated at day 21. (b) The expression of proteins was downregulated at days 14 and 21. (c) The expression of proteins was upregulated at days 14 and 21.
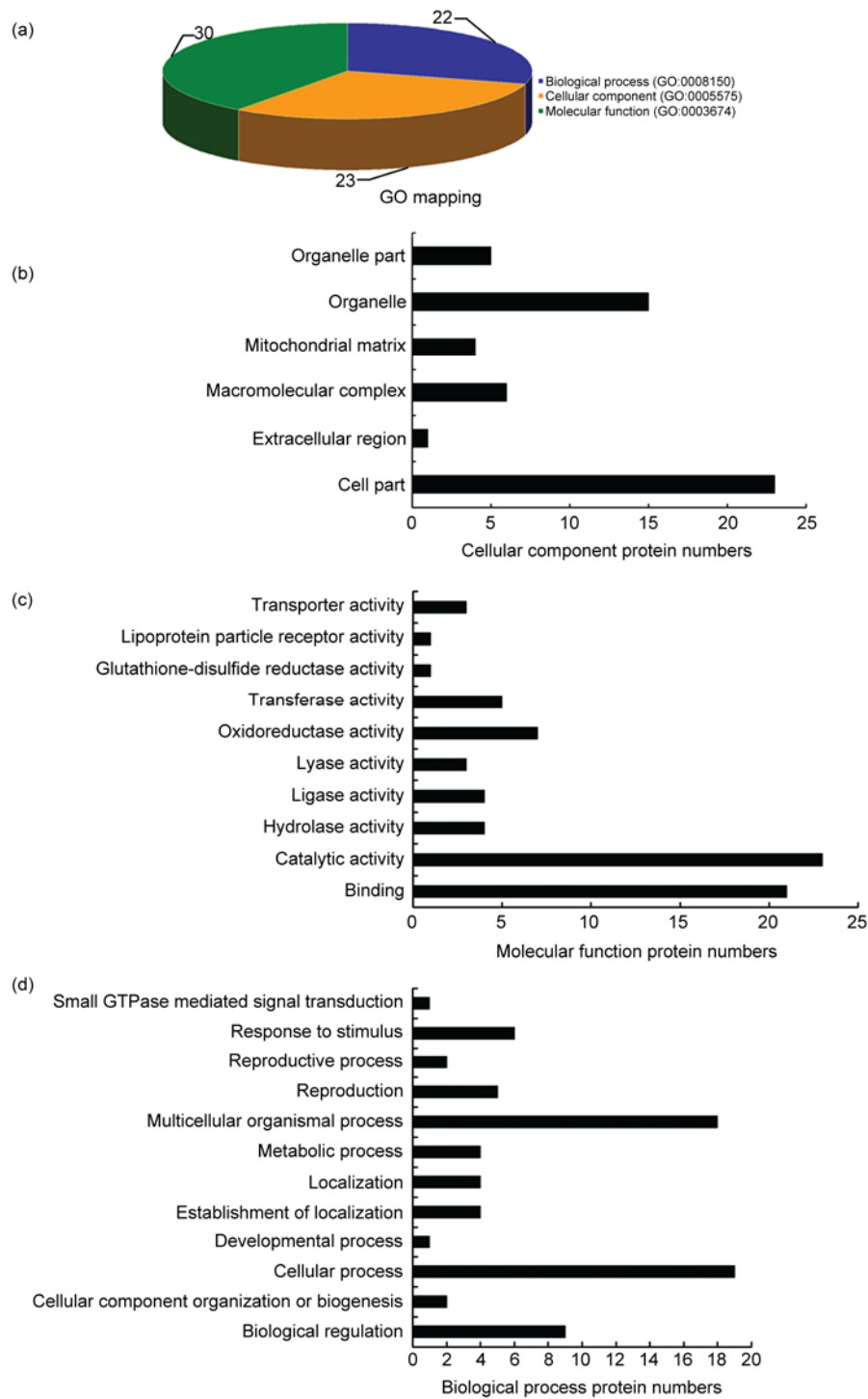
Figure 2   GO analyses of all differentially expressed proteins. (a) There are 23 proteins involved in cellular components, 30 proteins in molecular function, and 22 proteins in biological processes. (b) Protein numbers in the subgroup of cellular components. (c) Protein numbers in the subgroup of molecular function. (d) Protein numbers in biological processes.

2.4   Analyses of VCP protein

Protein-GO networks of all proteins are provided in Figure S1. Combining these results, we analyzed the interaction of proteins using an MAS (Molecular Annotation System). VCP (fold change at day 14 was 1.7281, and 1.2094 at day 21) interacted with many other proteins, suggesting that it plays an important role in the renal disease process. The VCP-GO networks are shown in Figure 3. The results indicated that HSPa5, markers of ERS, could interact with VCP via slac2a4 (omitted in Table 1). We also extracted the detailed GO function of VCP in Table 4, which showed that

Table 2 Cellular metabolic process related proteins

Uniprot AC	Protein name	Gene Ontology (GO)
P13221	AATC	2-oxoglutarate metabolic process; *L*-phenylalanine:2-oxoglutarate aminotransferase activity; axon terminus; biosynthetic process; carboxylic acid binding; cytosol; glutamate metabolic process; lysosome
Q9ER34	ACON	3 iron, 4 sulfur cluster binding; 4 iron, 4 sulfur cluster binding; aconitate hydratase activity; citrate hydro-lyase (*cis*-aconitate-forming) activity; citrate metabolic process; isocitrate hydro-lyase (*cis*-aconitate-forming) activity; isocitrate metabolic process
P10719	ATPB	ADP biosynthetic process; ATP binding; ATP hydrolysis coupled proton transport; ATP synthesis coupled proton transport; calcium ion binding; rotational mechanism; lipoprotein particle receptor activity; mitochondrial proton-transporting ATP synthase complex
Q920P0	DCXR	*D*-xylose metabolic process; *L*-xylulose reductase (NADP$^+$) activity; glucose metabolic process; membrane; nucleotide binding; protein homotetramerization; xylulose metabolic process
P48508	GSH0	glutamate metabolic process; glutamate-cysteine ligase activity; glutamate-cysteine ligase complex; glutathione biosynthetic process; negative regulation of neuron apoptosis; response to nitrosative stress; response to oxidative stress; soluble fraction
P19468	GSH1	ADP binding; anti-apoptosis; cell redox homeostasis; coenzyme binding; cysteine metabolic process; glutamate binding; glutamate metabolic process; glutathione biosynthetic process; response to heat; response to hormone stimulus; response to oxidative stress
P70619	GSHR	NADP binding; cell redox homeostasis; cytosol; flavin adenine dinucleotide binding; glutathione binding; glutathione metabolic process; glutathione-disulfide reductase activity; mitochondrion; protein homodimerization activity; soluble fraction; spermatogenesis
P41562	IDHC	2-oxoglutarate metabolic process; NAD binding; NADP binding; female gonad development; glyoxylate cycle; isocitrate dehydrogenase (NADP$^+$) activity; isocitrate metabolic process; magnesium ion binding; peroxisome; response to organic cyclic compound
P04182	OAT	N2-acetyl-*L*-ornithine:2-oxoglutarate 5-aminotransferase activity; mitochondrial matrix; ornithine metabolic process; ornithine-oxo-acid transaminase activity; pyridoxal phosphate binding
P13437	THIM	acetyl-CoA C-acyltransferase activity; acetyl-CoA metabolic process; anti-apoptosis; fatty acid beta-oxidation; mitochondrial matrix
Q3MIF4	XYLB	ATP binding; *D*-xylose metabolic process; xylulokinase activity
Q3MHS9	Q3MHS9	ATP binding; cytoplasm; protein folding; unfolded protein binding
D3ZZN3	D3ZZN3	AMP binding; acetate biosynthetic process; acetate-CoA ligase activity; propionate biosynthetic process
Q66HT1	Q66HT1	fructose-bisphosphate aldolase activity; glycolysis
B4F768	B4F768	1-pyrroline-5-carboxylate dehydrogenase activity; mitochondrial matrix; oxidoreductase activity, acting on the aldehyde or oxo group of donors, NAD or NADP as acceptor; proline biosynthetic process
Q68FT4	Q68FT4	ATP binding; succinate metabolic process; succinate-CoA ligase activity; succinyl-CoA metabolic process; tricarboxylic acid cycle

it likely has 14 functions, including ER to Golgi vesicle-mediated transport, proteasomal ubiquitin-dependent protein catabolism, and protein homooligomerization (Figure 3).

2.5 mRNA and protein expression of VCP and HSPa5 in the model

In the LC-MS/MS results, the expression of the two proteins at days 14 and 21 is shown in Figure 4(a), which includes groups B and C. To verify expression of the two proteins in the three groups, we detected the mRNA and protein expression level using real-time PCR and Western blotting. The results (Figure 4(b) and (c)) indicated that at days 14 and 21, the mRNA and protein expression level of VCP and HSPa5 were upregulated when compared to normal tissue. Although at day 21, the expression of VCP was downregulated, the difference between the two time points was not statistically significant.

2.6 Pathway analysis

All significant pathways in which these differentially expressed proteins were involved are shown in Figure S1 and Table 5. The main pathways include glutathione metabolism, reductive carboxylate cycle (CO_2 fixation), citrate cycle, arginine and proline metabolism, and control of genes including *Gclm*, *Gclc*, *Idh1*, *Gsr*, *Acss1*, *Aco2*, *Idh1*, *Suclg2*, *Aldh4a1*, *Oat*, and *Got1*. We obtained the correlation of these pathway related proteins/genes, as shown in Figure 4. VCP and HSPa5 were involved in the same pathways.

2.7 ERS of podocyte after inhibiting VCP

After treatment of MPCs with tunicamycin for 10 h, the expression level of HSPa5, the ERS marker, was upregulated, as shown in Figure 5. Expression of VCP also increased. If cell VCP was inhibited by siRNA, HSPa5 expression did not change. After the cell RNAi was treated

Table 3   Catalytic activity related proteins

Uniprot AC	Protein name	Gene Ontology (GO)
A2VCW9	AASS	mitochondrion; nucleotide binding; saccharopine dehydrogenase (NAD$^+$, *L*-glutamate-forming) activity; saccharopine dehydrogenase (NADP$^+$, *L*-lysine-forming) activity
P13221	AATC	2-oxoglutarate metabolic process; cytosol; glutamate metabolic process; lysosome; pyridoxal phosphate binding; soluble fraction
Q9ER34	ACON	3 iron, 4 sulfur cluster binding; 4 iron, 4 sulfur cluster binding; isocitrate metabolic process; mitochondrion; protein binding; tricarboxylic acid cycle
P10719	ATPB	ADP biosynthetic process; ATP binding; ATP hydrolysis coupled proton transport; mitochondrial proton-transporting ATP synthase complex, catalytic core F(1)
Q920P0	DCXR	*D*-xylose metabolic process; *L*-xylulose reductase (NADP$^+$) activity; glucose metabolic process; membrane; nucleotide binding; protein homotetramerization; xylulose metabolic process
Q64591	DECR	2,4-dienoyl-CoA reductase (NADPH) activity; mitochondrion
P48508	GSH0	glutamate metabolic process; glutamate-cysteine ligase activity; glutamate-cysteine ligase catalytic subunit binding; glutamate-cysteine ligase complex; glutathione biosynthetic process; negative regulation of neuron apoptosis; response to oxidative stress; soluble fraction
P19468	GSH1	ADP binding; anti-apoptosis; cell redox homeostasis; coenzyme binding; cysteine metabolic process; glutamate binding; glutamate-cysteine ligase complex; glutathione biosynthetic process; magnesium ion binding; negative regulation of neuron apoptosis; response to oxidative stress
P70619	GSHR	NADP binding; cell redox homeostasis; cytosol; flavin adenine dinucleotide binding; glutathione binding; glutathione metabolic process; glutathione-disulfide reductase activity; mitochondrion; protein homodimerization activity; soluble fraction; spermatogenesis
P41562	IDHC	2-oxoglutarate metabolic process; NAD binding; peroxisome; response to organic cyclic compound; response to steroid hormone stimulus; soluble fraction; tricarboxylic acid cycle
Q497B0	NIT2	nitrogen compound metabolic process; omega-amidase activity
P04182	OAT	N2-acetyl-*L*-ornithine:2-oxoglutarate 5-aminotransferase activity; mitochondrial matrix; ornithine metabolic process; ornithine-oxo-acid transaminase activity; pyridoxal phosphate binding
Q9WUW8	ST1C2	lysosome; sulfotransferase activity
P46462	TERA	ATP binding; ATPase activity; ER to Golgi vesicle-mediated transport; cytosol; endoplasmic reticulum; identical protein binding; lipid binding; microsome; nucleus; positive regulation of proteasomal ubiquitin-dependent protein catabolic process; protein homooligomerization; receptor binding
P13437	THIM	acetyl-CoA C-acyltransferase activity; acetyl-CoA metabolic process; anti-apoptosis; fatty acid beta-oxidation; mitochondrial matrix
P52759	UK114	endonuclease activity; mitochondrion; nucleus; peroxisome
Q3MIF4	XYLB	ATP binding; *D*-xylose metabolic process; xylulokinase activity
D4A2K1	D4A2K1	lyase activity
Q7TP54	Q7TP54	cellular iron ion homeostasis; ferric iron binding; oxidoreductase activity
D3ZZN3	D3ZZN3	AMP binding; acetate biosynthetic process; acetate-CoA ligase activity; propionate biosynthetic process
Q66HT1	Q66HT1	fructose-bisphosphate aldolase activity; glycolysis
B4F768	B4F768	1-pyrroline-5-carboxylate dehydrogenase activity; mitochondrial matrix; oxidoreductase activity, acting on the aldehyde or oxo group of donors, NAD or NADP as acceptor; proline biosynthetic process

with tunicamycin, the VCP expression level was lower than that of the group treated with only tunicamycin, but the HSPa5 expression level was significantly higher.

3   Discussion

Membranous glomerulonephritis (MGN) accounts for approximately 30% of cases of nephrotic syndrome in adults, with peak incidence between the ages of 30 and 50 years and a male to female ratio of 2∶1 [19]. Major contributions to our current understanding of the disease come from Heymann nephritis, a rat model of MGN [20]. The pathological features of membranous nephropathy are uniform and consistent incrassation of the glomerular capillary basement membrane, and diffuse subepithelial immune complex deposition. An obvious increase in proteinuria was observed in the pHN by day 14 and it peaked on day 21; on this day, interstitial fibrosis appeared [21]. Therefore, we selected days 14 and 21 as the two time points of the pHN model to analyze the differential protein expression profile using label-free LC-MS/MS. Proteomics applied at a large scale may provide useful diagnostic information. Several reports on MN have focused on the urine for diagnostic purposes
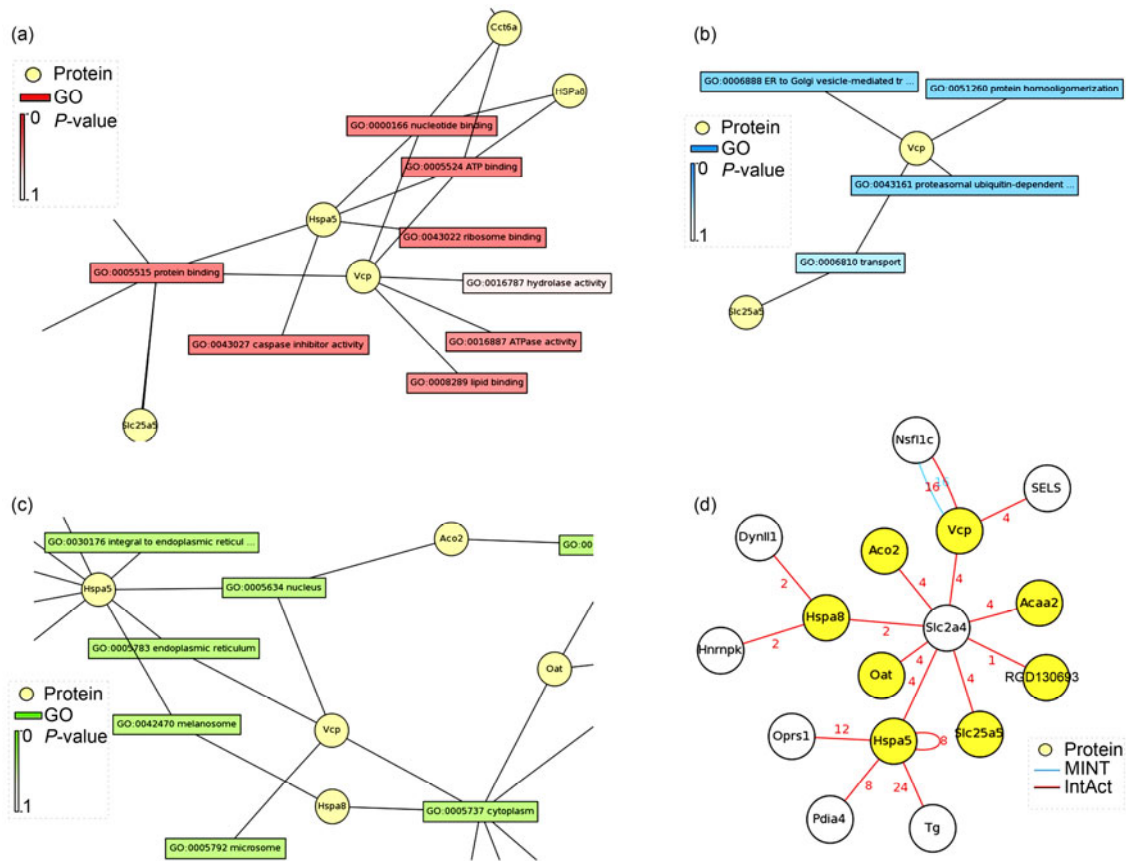
Figure 3 Protein-GO networks and interaction with VCP. (a) Significant molecular function network of VCP. (b) Significant biological process network of VCP. (c) Significant cellular component network of VCP. (d) Interaction graph of VCP; the numbers represent the frequency of interaction.
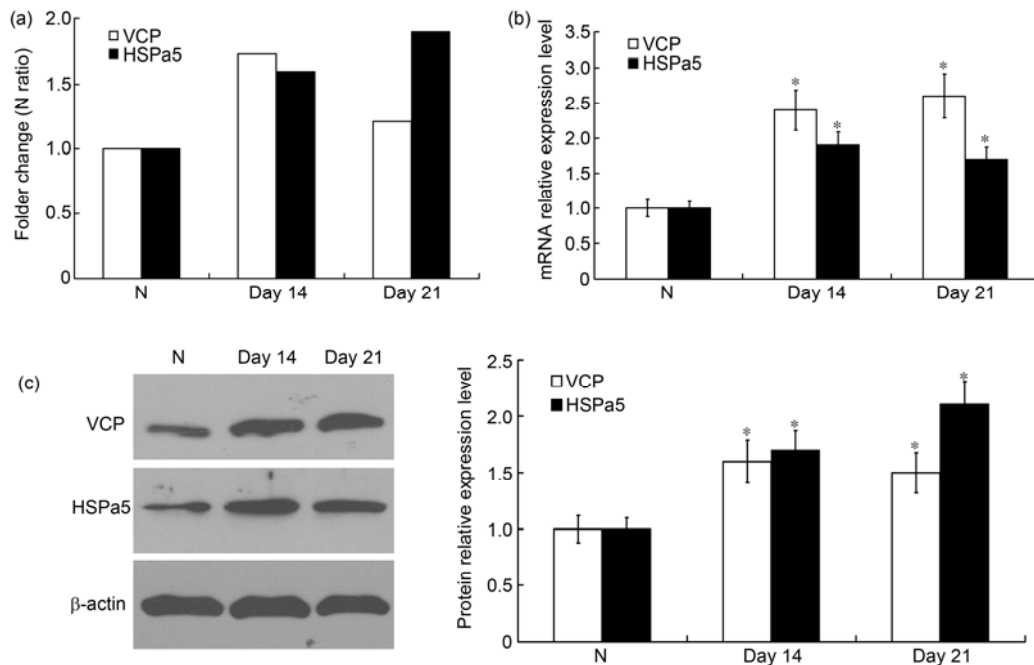

Figure 4 Verification of VCP and HSPa5 in LC-MS/MS by real-time PCR and Western blotting. (a) The degree of change of VCP and HSPa5 on days 14 and 21 in the pHN model detected by LC-MS/MS. (b) Real-time PCR determined the mRNA expression level of VCP and HSPa5; at days 14 and 21, the two proteins showed increased expression, and significant differences were observed between days 14 and 21 compared to normal tissue. *$P < 0.05$, $n = 3$. (c) Western blotting determined the protein expression level of VCP and HSPa5; at days 14 and 21, the two proteins showed increased expression, and significant differences were observed between days 14 and 21 compared to normal tissue. *$P < 0.05$, $n = 3$.

Table 4　The detailed GO analysis of VCP protein (GI:1786535)

Molecular function	Biological process	Cellular component
GO:0000166 nucleotide binding	GO:0006810 transport	GO:0005634 nucleus
GO:0005515 protein binding		GO:0005737 cytoplasm
GO:0005524 ATP binding	GO:0006888 ER to Golgi vesicle-mediated transport	GO:0005783
GO:0008289 lipid binding	GO:0043161 proteasomal ubiquitin-dependent protein catabolism	endoplasmic reticulum
GO:0016787 hydrolase activity	GO:0051260 protein homooligomerization	GO:0005792
GO:0016887 ATPase activity		microsome

Table 5　Pathway information of differentially expressed proteins[a]

Pathway	Count	P-value	Q-value	Gene	GI number
Glutathione metabolism	4	3.36×10^{-8}	1.68×10^{-8}	*Gclm*; *Gclc*; *Idh1*; *Gsr*	8393446; 25742748; 13928690; 1657632
Reductive carboxylate cycle (CO$_2$ fixation)	3	5.21×10^{-8}	2.08×10^{-8}	*Acss1*; *Aco2*; *Idh1*	157818027; 40538860;13928690
Citrate cycle (TCA cycle)	3	1.74×10^{-6}	5.81×10^{-7}	*Suclg2*; *Aco2*; *Idh1*	51260799; 40538860; 13928690
Arginine and proline metabolism	3	2.13×10^{-6}	6.08×10^{-7}	*Aldh4a1*; *Oat*; *Got1*	195540087; 11968102; 220684
Pentose phosphate pathway	2	1.63×10^{-4}	2.52×10^{-5}	*Aldob*; *Tkt*; *Aldob*	158081751; 149034221; 149020188
Glutamate metabolism	2	1.77×10^{-4}	2.52×10^{-5}	*Aldh4a1*; *Got1*	195540087; 220684
Alanine and aspartate metabolism	2	2.22×10^{-4}	2.62×10^{-5}	*Agxt2*; *Got1*	149027328; 220684
Propanoate metabolism	2	2.73×10^{-4}	3.03×10^{-5}	*Suclg2*; *Acss1*	51260799; 157818027
Glycolysis/Gluconeogenesis	2	0.002702	2.46×10^{-4}	*Acss1*; *Aldob*; *Aldob*	157818027; 158081751; 149020188
Antigen processing and presentation	2	0.002866	2.49×10^{-4}	*Hspa8*; *Hspa5*	13242237; 25742763
Alkaloid biosynthesis I	1	0.004703	3.62×10^{-4}	*Got1*	220684
Fatty acid elongation in mitochondria	1	0.007827	4.89×10^{-4}	*Acaa2*	18426866
Phenylalanine, tyrosine and tryptophan biosynthesis	1	0.007827	4.89×10^{-4}	*Got1*	220684
Glyoxylate and dicarboxylate metabolism	1	0.008607	4.92×10^{-4}	*Aco2*	40538860
Parkinson's disease	2	0.008613	4.92×10^{-4}	*Slc25a5*; *Atp5b*	32189350; 203033
Cysteine metabolism	1	0.010164	5.56×10^{-4}	*Got1*	220684
Phenylalanine metabolism	1	0.010942	5.61×10^{-4}	*Got1*	220684
Pentose and glucuronate interconversions	1	0.017142	7.79×10^{-4}	*Xylb*	76096348
Bile acid biosynthesis	1	0.018686	8.21×10^{-4}	*Acaa2*	18426866
Tyrosine metabolism	1	0.023305	9.51×10^{-4}	*Got1*	220684
Fructose and mannose metabolism	1	0.024839	9.94×10^{-4}	*Aldob*; *Aldob*	158081751; 149020188
Pyruvate metabolism	1	0.028666	0.001102553	*Acss1*	157818027
Fatty acid metabolism	1	0.031718	0.001185701	*Acaa2*	18426866
Glycine, serine and threonine metabolism	1	0.031718	0.001185701	*Agxt2*	149027328
Valine, leucine and isoleucine degradation	1	0.034759	0.001241406	*Acaa2*	18426866
Adherens junction	1	0.055052	0.001931646	*Actn4*	6636119
Leukocyte transendothelial migration	1	0.087242	0.002814248	*Actn4*	6636119
Tight junction	1	0.095122	0.002860587	*Actn4*	6636119
Systemic lupus erythematosus	1	0.105057	0.002959349	*Actn4*	6636119
Oxidative phosphorylation	1	0.117675	0.003159073	*Atp5b*	203033
Focal adhesion	1	0.137645	0.003536344	*Actn4*	6636119
Calcium signaling pathway	1	0.139006	0.003536344	*Slc25a5*	32189350
Regulation of actin cytoskeleton	1	0.149147	0.003699245	*Actn4*	6636119
Alzheimer's disease	1	0.178885	0.004160114	*Atp5b*	203033
MAPK signaling pathway	1	0.185356	0.004179774	*Hspa8*	13242237

a) P-value: we calculate the P value using a hypergeometric distribution. The genes are enriched significantly in the pathway when P value<0.05. Q value: Q is Fasle Discovery Rate (FDR), Q default 0.05, the less the Q is, the more significant the genes (or proteins) enriched in the one pathway (or GO term), and the less FDR.
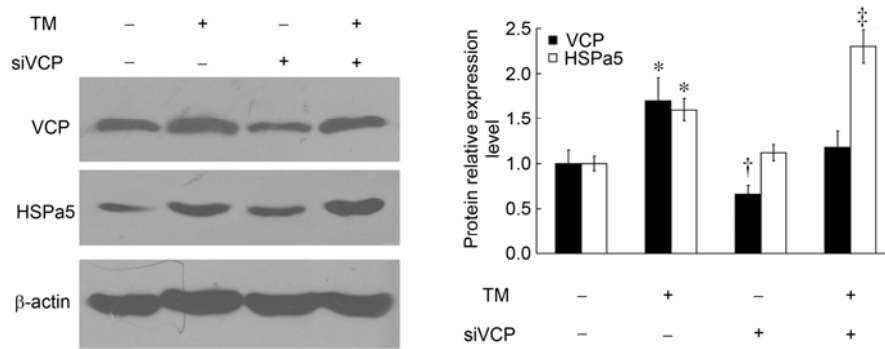
Figure 5   VCP was inhibited by RNAi, and ERS was induced by tunicamycin (Tm). MPCs were pretreated with 10 μg/mL Tm for 10 h to induce ERS; the expression levels of VCP and HSPa5 were both upregulated, and significant differences were observed compared with the control. $*P<0.05$, $n=3$. MPCs were transfected with siRNA and VCP protein expression was inhibited ($†P<0.05$, $n=3$), but HSPa5 expression did not change. Cells were transfected with siRNA of VCP and treated with Tm; HSPa5 expression increased, and a significant difference was observed between the Tm and Tm+siRNA groups ($‡P< 0.05$, $n=3$), although VCP expression was considerable in the control.

[22,23]. However, few reports have analyzed the differentially expressed proteins in the development of MN. Our objective was to identify the differentially expressed proteins seen in the pHN rat model. The results identified 41 differentially expressed proteins among three groups (day 0, day 14, and day 21). According to their expression changes, we divided them into three categories, A, B, and C. Proteins in group A were downregulated at day 14, but upregulated at day 21; group B showed downregulation at days 14 and 21; and group C showed upregulation at days 14 and 21. These proteins played an important role in the cellular process and biological regulation (listed in Table 1). The 16 proteins related to cellular metabolism were the predominant components. Since ERS profoundly affects metabolic processes [24], our findings strongly suggest that ERS on these proteins might be one of the most important biological events at day 14 or 21 in the PHN rat model. In the ERS process, misfolded protein in the ER would be degraded in the cytoplasm by catalytic proteins [25–27]. Table 3 lists the catalytic proteins (22) and their GO terms. These proteins affect the ERS process.

HSPa8 and HSPa5, the proteins needed for cellular metabolism, belong to the heat-shock protein family, and can bind to nascent polypeptides to facilitate correct folding [28,29]. They also function as an ATPase in the disassembly of clathrin-coated vesicles during transport of membrane components through the cell [30,31]. VCP, the catalytic protein, belongs to a family that includes putative ATP-binding proteins involved in vesicle transport and fusion, 26S proteasome function, and assembly of peroxisomes [32]. It also binds with clathrin and heat-shock protein Hsc70 to form a complex [33]. Additionally, it has been implicated in several other cellular events related to mitosis, including homotypic membrane fusion and ubiquitin-dependent protein degradation [34–36]. Our results indicate that most differentially expressed proteins could interact with each other, as shown in Figure 2, and among these, VCP could interact with HSPa8 or HSPa5 via slc2a4. Re-

grettably, our LC-MS/MS did not provide evidence of a significant change in slc24a expression. Our findings suggest that the cell processes mediated by VCP affect the development of MN.

Research indicates that the basic mechanism of MN is complement-mediated injury of the podocyte and its slit-pore membrane [37,38] and that ERS is the main cause of podocyte injury [39,40]. HSPa8 and HSPa5 are considered the markers of ERS increase [41–43], and VCP is an integral component of the ER-associated degradation and cellular stress pathways [44,45]. The detailed GO analysis of VCP in our study agreed with this finding (Table 4), and the pathway analyses showed VCP and HSPa5 to be in the same functional pathway. Therefore, we hypothesized that ERS, with VCP as a mediator, is an important trigger of podocyte injury in MN.

To test this theory, we cultured MPCs and induced ERS with tunicamycin, knocking down the expression level by RNAi. Results suggested when VCP of cells was knocked down under normal conditions, the ERS did not change, but VCP knockdown could increase ERS significantly after treatment with tunicamycin. Gp78-VCP interaction may represent one means of degradation of ER-associated degradation substrates [46]. VCP is required for maintenance of normal ER structure and function and mediates the degradation of certain proteins [47]. This supports our results that under normal conditions, the podocyte ERS is unaffected by VCP, but under stress, VCP may be activated to degrade unfolded proteins.

In conclusion, ERS plays an important role in podocyte injury of MN, and it is mediated via the HSPa5-VCP signaling pathway. In this process, the cellular metabolism proteins and catalytic proteins were predominant.

1   Sharpstone P, Ogg C S, Cameron J S. Nephrotic syndrome due to primary renal disease in adults: I. Survey of incidence in south east England. Br Med J, 1969, 2: 533–535

2   Rivera F, Lopez-Gomez J M, Perez-Garcia R. Clinicopathologic correlations of renal pathology in Spain. Kidney Int, 2004, 66: 898–904

3   Chen Z H, Qin W S, Zeng C H, et al. Triptolide reduces proteinuria in experimental membranous nephropathy and protects against C5b-9-induced podocyte injury *in vitro*. Kidney Int, 2010, 77: 974–988

4   Nangaku M, Pippin J, Richardson C A, et al. Beneficial effects of systemic immunoglobulin in experimental membranous nephropathy. Kidney Int, 1996, 50: 2054–2062

5   Jefferson J A, Pippin J W, Shankland S J. Experimental models of membranous nephropathy. Drug Discov Today Dis Models, 2010, 7: 27–33

6   Wu Q, Fan K, Sha W, et al. Highly sensitive detection of melamine based on reversed phase liquid chromatography mass spectrometry. Chin Sci Bull, 2009, 54: 732–737

7   Old W M, Meyer-Arendt K, Aveline-Wolf L, et al. Comparison of label-free methods for quantifying human proteins by shotgun proteomics. Mol Cell Proteomics, 2005, 4: 1487–1502

8   Asara J M, Christofk H R, Freimark L M, et al. A label-free quantification method by MS/MS TIC compared to SILAC and spectral counting in a proteomics screen. Proteomics, 2008, 8: 994–999

9   Dayarathna M K, Hancock W S, Hincapie M. A two step fractionation approach for plasma proteomics using immunodepletion of abundant proteins and multi-lectin affinity chromatography: Application to the analysis of obesity, diabetes, and hypertension diseases. J Sep Sci, 2008, 31: 1156–1166

10 Patel V J, Thalassinos K, Slade S E, et al. A comparison of labeling and label-free mass spectrometry-based proteomics approaches. J Proteome Res, 2009, 8: 3752–3759

11 Ke C Y, Geng X D. A new chromatographic method for fast separation of active proteins. Chin Sci Bull, 2008, 53: 1113–1116

12 Chant S, Katz A, Silverman M. Pathogenicity of a highly purified brush border membrane preparation in Heymann nephritis. J Clin Lab Immunol, 1980, 4: 133–140

13 Noble B, Van Liew J B, Andres G A, et al. Factors influencing susceptibility of LEW rats to Heymann nephritis. Clin Immunol Immunopathol, 1984, 30: 241–254

14 Bhan A K, Schneeberger E E, Baird L G, et al. Studies with monoclonal antibodies against brush border antigens in Heymann nephritis. Lab Invest, 1985, 53: 421–432

15 Shankland S J, Pippin J W, Reiser J, et al. Podocytes in culture: Past, present, and future. Kidney Int, 2007, 72: 26–36

16 Quan H, Peng X, Yang L, et al. An in-depth analysis of proteomics expression profiling in rat glomeruli utilizing LC-MS. Chin Sci Bull, 2010, 55: 2142–2151

17 Apweiler R, Bairoch A, Wu C H, et al. UniProt: The Universal Protein knowledgebase. Nucleic Acids Res, 2004, 32: D115–119

18 Yuan J S, Reed A, Chen F, et al. Statistical analysis of real-time PCR data. BMC Bioinformatics, 2006, 7: 85

19 Fauci A S, Braunwald E, Kasper D L, et al. Harrison's Principles of Internal Medicine. 17th ed. New York: McGraw-Hill, 2008. 1789–1790

20 Heymann W, Hackel D B, Harwood S, et al. Production of nephrotic syndrome in rats by Freund's adjuvants and rat kidney suspensions. Proc Soc Exp Biol Med, 1959, 100: 660–664

21 Bonegio R G, Fuhro R, Wang Z, et al. Rapamycin ameliorates proteinuria-associated tubulointerstitial inflammation and fibrosis in experimental membranous nephropathy. J Am Soc Nephrol, 2005, 16: 2063–2072

22 Weissinger E M, Wittke S, Kaiser T, et al. Proteomic patterns established with capillary electrophoresis and mass spectrometry for diagnostic purposes. Kidney Int, 2004, 65: 2426–2434

23 Ngai H H, Sit W H, Jiang P P, et al. Serial changes in urinary proteome profile of membranous nephropathy: Implications for pathophysiology and biomarker discovery. J Proteome Res, 2006, 5: 3038–3047

24 Wang X, Eno C O, Altman B J, et al. ER stress modulates cellular metabolism. Biochem J, 2011, 435: 285–296

25 Johnston J A, Ward C L, Kopito R R. Aggresomes: A cellular response to misfolded proteins. J Cell Biol, 1998, 143: 1883–1898

26 Katiyar S, Li G, Lennarz W J. A complex between peptide: *N*-glycanase and two proteasome-linked proteins suggests a mechanism for the degradation of misfolded glycoproteins. Proc Natl Acad Sci USA, 2004, 101: 13774–13779

27 Lilley B N, Ploegh H L. Multiprotein complexes that link dislocation, ubiquitination, and extraction of misfolded proteins from the endoplasmic reticulum membrane. Proc Natl Acad Sci USA, 2005, 102: 14296–14301

28 Tavaria M, Gabriele T, Anderson R L, et al. Localization of the gene encoding the human heat shock cognate protein, HSP73, to chromosome 11. Genomics, 1995, 29: 266–268

29 Yang Y, Turner R S, Gaut J R. The chaperone BiP/GRP78 binds to amyloid precursor protein and decreases Abeta40 and Abeta42 secretion. J Biol Chem, 1998, 273: 25552–25555

30 Heymann J B, Iwasaki K, Yim Y I, et al. Visualization of the binding of Hsc70 ATPase to clathrin baskets: Implications for an uncoating mechanism. J Biol Chem, 2005, 280: 7156–7161

31 Rapoport I, Boll W, Yu A, et al. A motif in the clathrin heavy chain required for the Hsc70/auxilin uncoating reaction. Mol Biol Cell, 2008, 19: 405–413

32 Pleasure I T, Black M M, Keen J H. Valosin-containing protein, VCP, is a ubiquitous clathrin-binding protein. Nature, 1993, 365: 459–462

33 Shi J, Dixon R A, Gonzales R A, et al. Identification of cDNA clones encoding valosin-containing protein and other plant plasma membrane-associated proteins by a general immunoscreening strategy. Proc Natl Acad Sci USA, 1995, 92: 4457–4461

34 Nagahama M, Suzuki M, Hamada Y, et al. SVIP is a novel VCP/p97-interacting protein whose expression causes cell vacuolation. Mol Biol Cell, 2003, 14: 262–273

35 Heo J M, Livnat-Levanon N, Taylor E B, et al. A stress-responsive system for mitochondrial protein degradation. Mol Cell, 2010, 40: 465–480

36 Tresse E, Salomons F A, Vesa J, et al. VCP/p97 is essential for maturation of ubiquitin-containing autophagosomes and this function is impaired by mutations that cause IBMPFD. Autophagy, 2010, 6: 217–227

37 Cunningham P N, Hack B K, Ren G, et al. Glomerular complement regulation is overwhelmed in passive Heymann nephritis. Kidney Int, 2001, 60: 900–909

38 Glassock R J. The pathogenesis of idiopathic membranous nephropathy: A 50-year odyssey. Am J Kidney Dis, 2010, 56: 157–167

39 Inagi R, Nangaku M, Onogi H, et al. Involvement of endoplasmic reticulum (ER) stress in podocyte injury induced by excessive protein accumulation. Kidney Int, 2005, 68: 2639–2650

40 He F, Chen S, Wang H, et al. Regulation of CD2-associated protein influences podocyte endoplasmic reticulum stress-mediated apoptosis induced by albumin overload. Gene, 2011, 484: 18–25

41 Lai M T, Huang K L, Chang W M, et al. Geldanamycin induction of grp78 requires activation of reactive oxygen species via ER stress responsive elements in 9L rat brain tumour cells. Cell Signal, 2003, 15: 585–595

42 Matthews J A, Belof J L, Acevedo-Duncan M, et al. Glucosamine-induced increase in Akt phosphorylation corresponds to increased endoplasmic reticulum stress in astroglial cells. Mol Cell Biochem, 2007, 298: 109–123

43 Kammoun H L, Chabanon H, Hainault I, et al. GRP78 expression inhibits insulin and ER stress-induced SREBP-1c activation and reduces hepatic steatosis in mice. J Clin Invest, 2009, 119: 1201–1215

44 Vij N, Fang S, Zeitlin P L. Selective inhibition of endoplasmic reticulum-associated degradation rescues DeltaF508-cystic fibrosis transmembrane regulator and suppresses interleukin-8 levels: Therapeutic implications. J Biol Chem, 2006, 281: 17369–17378

45 Lass A, McConnell E, Nowis D, et al. A novel function of VCP (valosin-containing protein; p97) in the control of *N*-glycosylation of proteins in the endoplasmic reticulum. Arch Biochem Biophys, 2007, 462: 62–73

46 Zhong X, Shen Y, Ballar P, et al. AAA ATPase p97/valosin-containing

protein interacts with gp78, a ubiquitin ligase for endoplasmic reticulum-associated degradation. J Biol Chem, 2004, 279: 45676–45684

47   Wojcik C, Rowicka M, Kudlicki A, et al. Valosin-containing protein (p97) is a regulator of endoplasmic reticulum stress and of the degradation of N-end rule and ubiquitin-fusion degradation pathway substrates in mammalian cells. Mol Biol Cell, 2006, 17: 4606–4618

Supporting Information

Figure S1   Protein-GO networks of all proteins.

The supporting information is available online at csb.scichina.com and www.springerlink.com. The supporting materials are published as submitted, without typesetting or editing. The responsibility for scientific accuracy and content remains entirely with the authors.